THE PUBLISHING HOUSE
OF THE ROMANIAN ACADEMY

PROCEEDINGS OF THE ROMANIAN ACADEMY, ***Series A,***
Volume 18, Number 1/2017, pp. 72–80

EXPERIMENTAL VALIDATION OF ACOUSTIC MODES FOR FLUID STRUCTURE COUPLING IN THE CAR HABITACLE

Iulian LUPEA

Technical University of Cluj-Napoca
E-mail: iulian.lupea@mep.utcluj.ro

Abstract. In the paper the acoustic and structural modes of vibration of a fluid - structure coupled system (a car cabin) are under observation. Firstly a system of a structural mass - spring - damper on one side and a tube filled with air on the other side is investigated. The natural frequencies of both uncoupled subsystems are observed in parallel to the natural frequencies of the coupled system. A simplified car cabin is observed, in order to calculate frequency response functions like the one between the resulted pressure in the cavity and the structural excitation of the firewall. Acoustic modes and structural modes of vibration by using the finite element analysis are derived. The validation of some acoustic modes in terms of the natural frequencies and the pressure distribution has been observed by using an experimental approach in which the pressure variation along important directions is traced.

Key words: acoustic modes, structural modes, fluid-structure coupling, natural frequencies of the coupled system, acoustic mode validation, frequency response functions.

1. INTRODUCTION

The reduction of the interior vibrations and noise in automobile passenger compartment is of continuous interest. Noise and vibrations are generated from sources like the engine, transmission or driveline, wind, the exhaust system and from the tires-road contact. These perturbations are transmitted through the body structure and the air to the comfort points on the passenger compartment, degrading the acoustic comfort in the habitacle. The acoustics of the compartment is as well determined by the structural modal characteristics and the acoustic modal characteristics of the cabin and on the other side by the nature of the coupling between the structural and the acoustic subsystems. For the coupled air-structure analysis an elementary air-structure system has been considered in order to enrich the perception on the coupling effect [4]. This system is similar to the coupling between a body in white structural panel and the air of the passenger compartment. In the sequel, the study is focused on the low frequency noise (under 300 Hz), of a wooden box considered as a simplified car passenger compartment model which has been manufactured [1] for simulations and experimental purposes. The pannels vibration will generate an important part of the automobile interior noise. Firstly the structural and the acoustic systems will be considered separately and a normal modes analysis will be performed on each subsystem. Later in the finite element analysis the coupling of the two subsystems will be considered and the modal synthesis method is used in order to reduce the number of degrees of freedom of the coupled system and the computation effort. The differential equations of the coupled air - structure and damped system is written as follows [8, 10, 12, 13]:

$$\begin{bmatrix} M_s & 0 \\ -A_{sf}^T & M_p \end{bmatrix}\begin{bmatrix} \ddot{Q}_s \\ \ddot{Q}_p \end{bmatrix}+\begin{bmatrix} C_s & 0 \\ 0 & C_p \end{bmatrix}\begin{bmatrix} \dot{Q}_s \\ \dot{Q}_p \end{bmatrix}+\begin{bmatrix} K_s & A_{sf} \\ 0 & K_p \end{bmatrix}\begin{bmatrix} Q_s \\ Q_p \end{bmatrix}=\begin{bmatrix} f_s \\ f_p \end{bmatrix}, \tag{1}$$

where: Q_s, Q_p are the structural nodal displacement (a×1) and acoustic nodal pressure (b×1) vectors, f_s, f_p are the external force excitation vectors applied on the structure (the firewall for instance) and the external sound pressure vector applied on the air domain (like a loudspeaker source) respectively. M_s, C_s

and K_s are the structural mass, damping and stiffness (a × a) matrices. M_p, C_p, K_p are the acoustic mass, damping and rigidity ($b \times b$) matrices. The matrix A_{sf} describes the spatial coupling between the acoustic and structure domains. The term A_{sf}^T transforms the structural accelerations into sound pressure (excitation) on the acoustic cavity and A_{sf} transforms the air pressure into forces acting on the structure. Integer numbers *a* and *b* are the numbers of degrees of freedom for the structure nodes and the fluid nodes respectively.

The trimmed body and seats can be neglected at this stage. At low frequencies the acoustic wavelength is greater then the seat thickness, hence the absorption can be neglected. For a real vehicle structure simulation, simplifications are also present when additional components (seats, accessories), can be taken in consideration by using their participation in the mass and stiffness matrix. Therefore, in the finite element model one can use concentrated masses or non-structural masses which can be connected with constraints to the model, simulating the real connection of these parts. Also, we will be looking for acoustic results due to the movement of the structural panels of the body in white. The car structure dynamical model based on resonant frequencies, damping ratios and mode shapes is the target of the structural modal analysis [11, 13]. In the design of the body in white (BIW), which transfers the excitation from the main sources, the frequency response analysis based on frequency response functions is essential.

2. ONE DIMENSIONAL AIR-STRUCTURE COUPLING – ANALITICAL SOLUTION

The simplified model observed in the sequel is similar to the coupling between a sheet metal panel of the body in white and the air of the car cabin. In case one of the natural frequencies of the enclosure equals or is close to a natural frequency of the air in the cabin, the excitation at the resonance will happen. In order to analytically observe the coupling or interaction between a volume of air and the elastic enclosure, the elementary system shown in Fig. 1 is considered. The straight tube is assumed elastic at one end and acoustically rigid at the opposite end. The structure elasticity is modeled by a single degree of freedom mass-spring-damper system. The elastic end of the tube can be seen like a flat piston of section area *A* (a diameter being less than the sound wavelength) and mass m_s, which displacement *u(t)* is small about the static position. The natural frequency f_{s0} associated to the structure subsystem and natural frequencies $f_{f,n}$ associated to the fluid subsystem, would be:

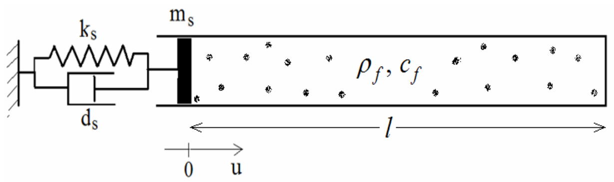

Fig. 1 – One d.o.f. structure coupled with the air of a tube.

$$f_{s0} = 1/2\pi \cdot \sqrt{k_s / m_s} \quad ; \quad f_{f,n} = c_f / 2l \cdot n, \quad n = 1, 2, 3, \ldots \tag{2–3}$$

where k_s and m_s are the spring stiffness and respectively the piston mass, c_f is the sound velocity in air, *l* is the length of the air column filling the tube and *n* is the acoustic mode index [7].

In order to determine the natural frequencies of the coupled system the differential equation of each subsystem influenced by the other one, has to be written [4, 10]. The derivation in details of the process of the determination of the natural frequencies of the coupled air-structure system can be found in [4]. The following transcendental equation is obtained:

$$\tan(2\pi l f / c_f) = A Z_0 f / [2\pi m_s (f^2 - f_{s0}^2)] . \tag{4}$$

The solutions f_i, $i = 1,2,3,\ldots$ of the equation (4) are the natural frequencies of the structure-air coupled system. The left member of (4) equals zero for πn radians (n = 1, 2, 3…) of the argument of the tangent function: $2lf / c_f = n$, resulting the known (3) relation that gives the eigenvalues $f_{f,n}$ of the fluid

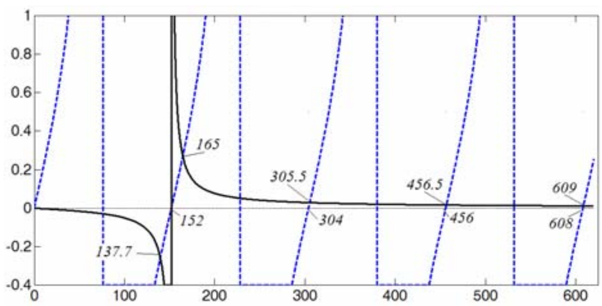

Fig. 2 – M_s = 0.01 and k_s = 9122.

subsystem with rigid ends. The right member of the equation (4) has a null denominator for $f = f_{s0}$. This member increases asymptotically to +∞ for the argument f decreasing to f_{s0} and tends asymptotically to -∞ for f increasing to f_{s0}. Let us consider a spring-mass-tube system with the same value of 152 Hz for the first natural frequency of each of the two uncoupled subsystems. This is realized for the following system characteristics [SI]: $M_s = 0.01$, $k_s = 9\ 122$, $L =$ 1.13 152, $A = 0.001$.

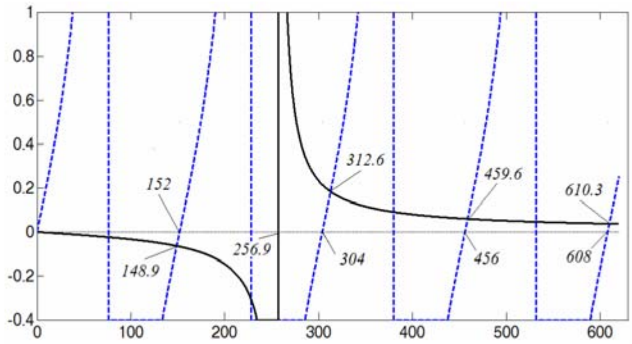

Fig. 3 – $M_s = 0.0035$ and $k_s = 9122$.

The natural frequencies 137.7Hz, 165Hz, 305.5Hz etc. of the coupled system are obtained graphically by using Matlab and are shown in Fig. 2. The solutions are placed at the multiple intersections between the two curves, one associated to the left and the second associated to the right member of the equation (4). The first natural frequency $f_i = 137.7$ Hz of the coupled system will be different from the unique natural frequency $f_s = 152$ Hz of the mass-spring subsystem that equals the first natural frequency of the air in the tube $f_{f,1} = 152$ Hz. All subsequent frequencies originating from the air in the tube will be a little different from the associated acoustic mode order $i = 2, 3,\ldots$, of the tube with rigid ends, as one can observe in row no. 1 of Table 1. The eigenvalue of the spring-mass subsystem can be close to a higher eigenvalues of the air in tube or between to adjacent eigenvalues. Hence, for a smaller piston mass the natural frequency of the mass-spring subsystem increases and the associated curve is shifting to the right with regards to the right member graph, in the graph. The abscissa of the intersection points are changing like for example in Fig. 3 and the associated row no. 2 of Table 1, where the intersection point is at the natural frequency $f_2 = 251.8$ Hz and $y = -1.815$ is not visible in the figure. As far as the natural frequency of the spring-mass subsystem is next to a natural frequency of the tube with rigid walls subsystem, the tube natural frequency is replaced with two different natural frequencies of the coupled system.

Table 1

$L = 1.13152$; $A = 0.001$; $\rho_f = 1.205$; $c_f = 344$				
	M_s k_s	Mass-spring: f_s	Tube with air, rigid ends [Hz] $f_{f,n}$, $n = 1,\ldots,4$	Coupled system [Hz] f_i, $i = 1, 2, 3$...
1	0.01, 9122	152.	152, 304 456, 608	137.7, 165, 305.5, 456.5, 609
2	0.0035, 9122	256.9	152, 304, 456, 608	148.9, 251.8, 312.6, 459.6, 610.3

3. CABIN MODAL ANALYSIS SIMULATION

3.1. The eigenvalue problem of the coupled system and the finite element model

The eigenvalue problem of the coupled system is obtained from (1) by neglecting the exterior forces, the damping and by assuming a harmonic solution for the dynamics of the whole system:

$$\begin{bmatrix} K_s & A_{sf} \\ 0 & K_p \end{bmatrix} \begin{bmatrix} \Lambda_{si} \\ \Lambda_{pi} \end{bmatrix} = \omega_i^2 \begin{bmatrix} M_s & 0 \\ -A_{sf}^T & M_p \end{bmatrix} \begin{bmatrix} \Lambda_{si} \\ \Lambda_{pi} \end{bmatrix}, \; i = 1,\ldots, a+b, \tag{5}$$

where $[\ \Lambda_{si}\ \Lambda_{pi}\ ]^T$ is the eigenvector of mode i of the coupled system (composed from the structural or shape vector and the fluid or pressure distribution vector) associated to the natural frequency ω_i of the coupled system. Integer numbers a, b are the number of degrees of freedom for the structure and the fluid respectively. For large systems like the car cabin, solving the system is performed with high computational effort, hence the component modal synthesis (CMS) method [3] is preferred. The coupled eigenmodes when using the CMS approach are expressed in terms of the eigenvectors of the two subsystems: the cavity and the fluid considered uncoupled.

The interior side of the box is meshed by using structural triangular shell elements. The interior volume occupied by the air is meshed by using tetrahedral volume elements. Each node of the air has only one degree of freedom, expressing the air pressure. The maximum number of the observed acoustic modes is dictated by the mesh size. The wavelength of an acoustic mode is longer than the wavelength of a mode of the structural panels at a comparable frequency, hence the mesh of the air can be in general coarser than the mesh of the enveloping structure. The box considered is made of 18 mm thick compressed sawdust PAL of 0.74e-9 [t/mm^3] the density, the Young modulus of 3 600 [N/mm^2] and the Poisson ratio is 0.25. The elastic modulus has been experimentally determined. In the first approach the cavity walls are considered rigid when the air pressure is acting on them. A material model like MAT10, available on various solvers like Nastran, Optistruct or Radioss, has been used to model the air (ρ = 1.18e–12t/mm^3, c = 3.46e5mm/s at 25C^o). The firewall made of a sheet of steel is modelled by shell elements. The goal is to determine reduced sets of eigenmodes separately for the fluid and the structure to be used in the frequency response analysis.

The reduced set of modal shapes is employed as sets of basis vectors or modes when the component modal synthesis (CMS) method is used. When using the CMS method the structural modes Λ_{s0i} , i = 1,…, ra have to be determined by using the finite element analysis, by solving the following eigenvalue equation:

$$[K_s][\Lambda_{s0i}] = \omega_{s0i}^2 [M_s][\Lambda_{s0i}],\ i = 1,\ldots, ra. \tag{6}$$

The (rigid wall) acoustic modes Λ_{p0i} , are determined by solving the eigenvalue equation (7):

$$[K_p][\Lambda_{p0i}] = \omega_{p0i}^2 [M_p][\Lambda_{p0i}],\ i = 1,\ldots, rb. \tag{7}$$

The first (reduced) number of structural and fluid eigenvectors is retained only.
The modal matrices $\Lambda_{s0} = [\Lambda_{s01}\ \Lambda_{s02},\ldots,\Lambda_{s0ra}]$ and $\Lambda_{p0} = [\Lambda_{p01}\ \Lambda_{p02},\ldots,\Lambda_{p0rb}]$ from the structure and the fluid subsystems will be used to express the structural nodal displacements and acoustic nodal pressures (Q_s, Q_p) in function of several (ra and rb respectively) modal coordinate vectors:

$$\{Q_s\} = [\Lambda_{s0}]\{\xi_s\} \text{ and } \{Q_p\} = [\Lambda_{p0}]\{\xi_p\}. \tag{8}$$

The relations (8) are substituted in (1), then relation (1) is premultiplied by modal matrices (9):

$$\begin{bmatrix} [\Lambda_{s0}]^T & [0] \\ [0] & [\Lambda_{p0}]^T \end{bmatrix} \tag{9}$$

resulting:

$$\begin{bmatrix} m_s & 0 \\ -a_{sf}^T & m_p \end{bmatrix}\begin{bmatrix} \ddot{\xi}_s \\ \ddot{\xi}_p \end{bmatrix} + \begin{bmatrix} c_s & 0 \\ 0 & c_p \end{bmatrix}\begin{bmatrix} \dot{\xi}_s \\ \dot{\xi}_p \end{bmatrix} + \begin{bmatrix} k_s & a_{sf} \\ 0 & k_p \end{bmatrix}\begin{bmatrix} \xi_s \\ \xi_p \end{bmatrix} = \begin{bmatrix} \Lambda_{s0}^T f_s \\ \Lambda_{p0}^T f_p \end{bmatrix} \tag{10}$$

where: $$m_s = \Lambda_{s0}^T M_{s0} \Lambda_{s0},\quad c_s = \Lambda_{s0}^T C_{s0} \Lambda_{s0},\quad k_s = \Lambda_{s0}^T K_{s0} \Lambda_{s0},\quad a_{sf} = \Lambda_{s0}^T A_{sf} \Lambda_{p0} \tag{11}$$

$$-a_{sf}^T = -\Lambda_{p0}^T A_{sf}^T \Lambda_{s0},\ m_p = \Lambda_{p0}^T M_{p0} \Lambda_{p0},\ c_p = \Lambda_{p0}^T C_{p0} \Lambda_{p0},\ k_p = \Lambda_{p0}^T K_{p0} \Lambda_{p0}. \tag{12}$$

The air pressure at the comfort points [8] is important for the acoustic quality of the habitacle. Hence, the harmonic excitation/ harmonic response is important to evaluate the fluid mode participation and the structure mode participation at these response (comfort) spots of the cabin, which can be evaluated for each frequency of excitation. After delimiting the habitacle panels, the panel participation can be evaluated.

3.2. Acoustic modal analysis by simulation – rigid enclosure/walls

In order to have some reference values for the modal parameters, the eigenvalues of the air in a rectangular cavity, has been considered. The natural frequencies [7] are (13):

$$f_{n_x,n_y,n_z} = (c_0/2)[(n_x/l_x)^2 + (n_y/l_y)^2 + (n_z/l_z)^2]^{1/2} \tag{13}$$

and the associated acoustic mode shapes or pressure distribution are calculated by using the relation (14):

$$p(x,y,z,t) = p_0 \cos(\pi\, n_x \cdot x / l_x) \cos(\pi\, n_y \cdot y / l_y) \cos(\pi\, n_z \cdot z / l_z) \sin(\omega t)\,, \tag{14}$$

where n_x, n_y, n_z are integer numbers and the real variables x, y, z are limited by the box geometry:

$$0 \le x \le l_x\,,\;\; 0 \le y \le l_y\,,\;\; 0 \le z \le l_z\,. \tag{15}$$

The natural frequencies and the associated acoustic mode shapes of the simplified enclosure, were obtained by using Optistruct [13]. The simplified parallelepiped enclosure is characterised by the following relations:

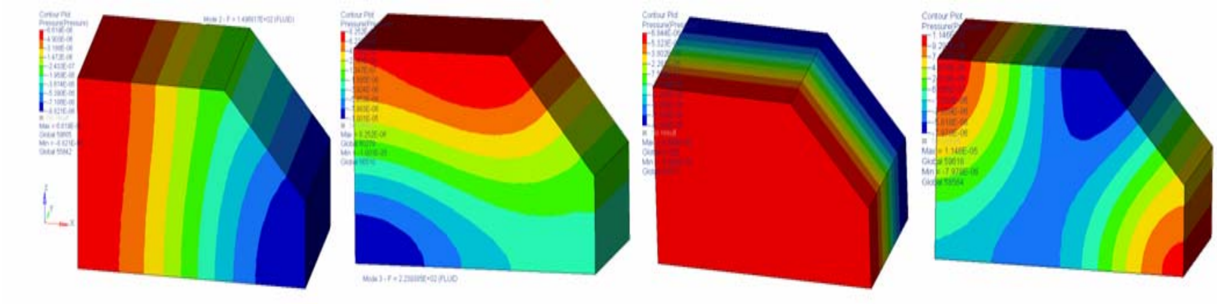

Fig. 4 – M # 2: 152 Hz [100], M # 3: 226 Hz [001], M # 4: 245 Hz [010] and M # 5: 273 Hz [200].

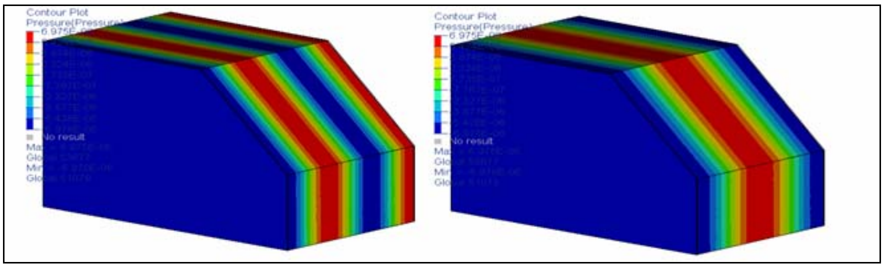

Fig. 5 – Modes 494 Hz [020] and 729 Hz [030].

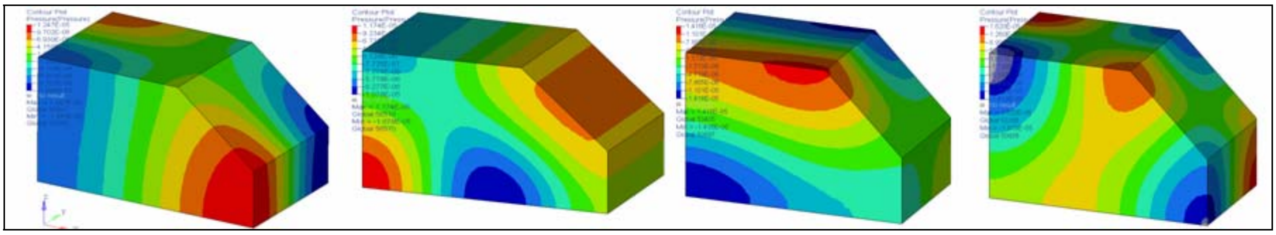

Fig. 6 – M # 6: 285 Hz [110], M # 7: 321 Hz [2’00], M # 8: 333 Hz [011] and M # 9: 365 Hz [210].

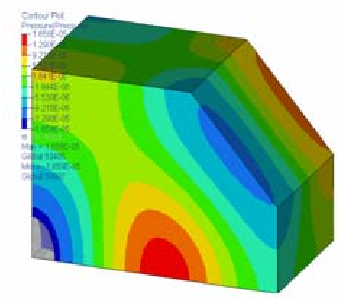

Fig. 7 – 403 Hz [2’10].

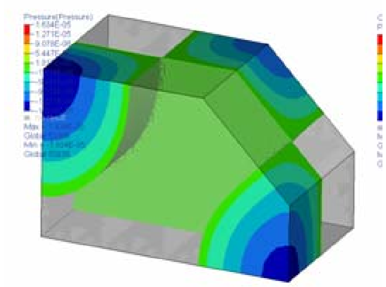

Fig. 8 – M # 9, 365 [210].

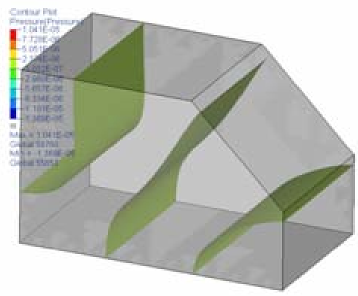

Fig. 9 – M # 10 392 [300].

$l_x > l_z > l_y$. For the enclosure’s acoustic modes, we will employ the notation (*nx*, *ny*, *nz*), where *nx*, *ny*, *nz* = 0, 1, 2… which is specific to the rectangular volumes. One can observe axial acoustic modes of the type (*nx*, 0, 0), (0, *ny*, 0) or (0, 0, *nz*), tangential modes of the type (*nx*, *ny*, 0), (*nx*, 0, *nz*) or (0, *ny*, *nz*) and oblique or three-dimensional modes (*nx*, *ny*, *nz*). Let us take a look at the modal pressure distribution for some of the acoustic modes. The first acoustic mode, with the lowest frequency of 152 Hz, is the axial mode [100] with pressure distribution shown in Fig. 4/ M#2. For this mode all the air particles are oscillating approximately along OX axis (excepting the particles at the maximum pressure resting on the opposite walls). The zero pressure surface is about at the middle section of the length l_x of the enclosure. The frequency of 226 Hz is associated to the air particle vibration in the first vertical acoustic mode [001], approximately along the height (OZ axis) and depicted in Fig. 4/ M#3. The third acoustic mode (Fig. 4 /M#4) at 245 Hz, is along the OY axis [010]. The modes along OY axis can be exactly calculated by using a reduced form of the expression (13) associated to the rectangular enclosure: $f_{0,n_y,0} = c_0 / 2 \cdot n_y / l_y$. The pressure amplitude is observing the relation:

$$p(y) = C_{0,n_y,0} \cos(\pi n_y \cdot y / l_y) \quad (16).$$

For $y = 0$ and $y = l_y$, at the two opposite parallel walls the alternating pressure has maximal amplitudes of $\pm C_{0,n_y,0}$ (same sign or opposite sign).

For $y = l_y/2$ and mode [010] at the mid plane the pressure is zero and the displacement amplitude of the air particles is maximal. Two higher modes [020] and [030] in which the air is vibrating along OY axis are shown in Fig. 5. The second and the third axial acoustic modes along OX axis [200], [300] are depicted in Fig. 4 M#5 and Fig. 9, where one can observe two and respectively three surfaces of zero relative pressure.

A different axial OX mode [2’00] at 321 Hz, can be seen in Fig. 6/ M#7 in which the air is vibrating between the low-left corner and the windscreen. This mode is a different one when comparing with mode [200], in which the air is moving between the upper-left corner and the firewall. Tangential acoustic modes are [110] where the air is vibrating simultaneously along OY and OX and [011] where the air is moving along OY and OZ directions.

A higher tangential mode [210] (Fig. 6 and Fig. 8) has two zero pressure surfaces along OX direction and one along OY direction. In the mode [2’10] depicted in Fig. 7 (similar to [210] mode) the air is vibrating normal to the windshield. Various other acoustic modes are resulting from the simulation with a more complicated pressure variation; the higher the mode in general the more complicated the pressure distribution is.

3.3. Modal analysis simulation separately for the structure

The whole structure is placed on top of a thick layer of soft foam. The modal analysis simulation is performed free of constrains. The firewall is modeled by a steel plate of 1.2 mm thick, $E = 2.1\text{e}5$MPa, density 7.9e–9 t/mm^3 and $\mu = 0.3$. In the first two modes (S#1, S#2) a central zone of the firewall is moving with relative large amplitude. In the third mode (75 Hz) two areas of the firewall are moving out of phase. In the fourth mode mainly the lateral panels are moving in phase. In the fifth mode mainly three panels undergo vibratory motion: when the base panel is moving up the lateral faces are decreasing the distance between them and vice versa (Fig. 10, S#5). These structural modes are placed under the first acoustic mode frequency.

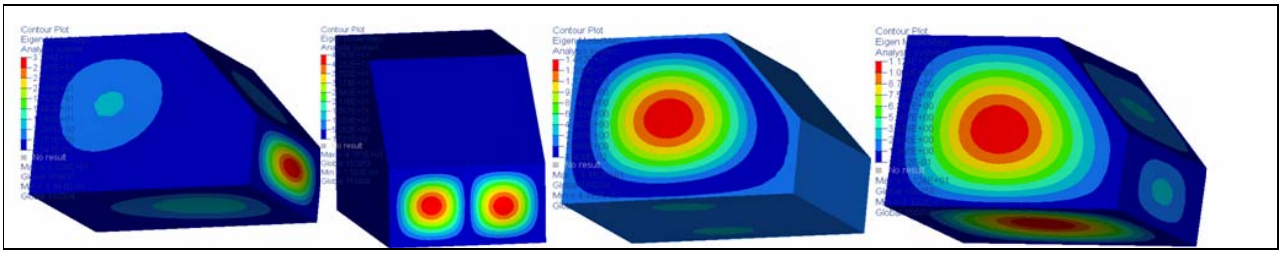

Fig. 10 – Structure modes: S # 1,2 (56 Hz,58 Hz), S # 3 (75 Hz), S # 4 (77 Hz), S # 5 (83 Hz).

Some structural modes have the frequency very close to an acoustic mode, like the mode 28 (227 Hz) and the acoustic mode 3 (226 Hz [001]), when the acoustic mode is excited by the proper panel of the structural mode. In reality, like has been shown in the one dimensional air-structure coupling, new modes of the whole coupled system will be present (Table 1). For the coupled fluid-structure system, the panels individual contribution to the interior pressure at the comfort points is of interest, hence finding the “noisy” panels. For the present structure an electromagnetic shaker has been used to excite harmonically or randomly the steel panel (firewall). The force exciting the panel is measured by a force sensor and the acceleration exciting the fluid domain at the boundary can be known. It is useful to find the contribution of each surrounding panel to the sound pressure at the comfort points, contribution expressed by the amplitude and the phase of the pressure vector. By drawing a polar amplitude-phase diagram [10] for a unique frequency excitation one can observe the importance of each panel like the windscreen, back window, doors, front or rear floor, roof etc. to the cavity spot of interest. From the phase of the total pressure and the contributing panels one can predict if the decrease of a panel contribution really is decreasing the resultant pressure or is by contrary increasing the noise at the spot of interest.

4. EXPERIMENTAL VALIDATION OF ACOUSTIC MODES

At the beginning frequency response functions (FRF) are measured. The simplified enclosure has two detachable walls, one is placed in a vertical plane at the firewall place and the second one is horizontal at the roof level. A microphone can slide inside the box along profiled bars anchored on the box walls following the selected orientation. The position of the microphone along the bar can be changed from outside the box, by using marked ribbons. An accelerometer (1.5 g) is attached to the loudspeaker cone. The loudspeaker is used to excite the air in the box, the accelerometer is monitoring the vibration of the loudspeaker cone and the microphone is evaluating the pressure level. The acquisition system consists of a dynamic signal acquisition board (NI, PCI-4451), a signal conditioning unit and Labview software applications for measuring FRFs. One channel is used to excite the loudspeaker and two simultaneous sampling input channels to acquire signals coming from the accelerometer and the microphone. At this stage the enclosure is all around bounded by the sawdust compressed boards. During the measurements the microphone has been placed in horizontal position and away from the cavity boundaries at a minimum of 15mm. The loudspeaker is placed on the floor of the test cavity and is oriented along the axis of interest. Various FRFs between the microphone and the accelerometer have been measured by using a swept sine sound wave excitation in the range 100 Hz to 500 Hz or random excitation. The peaks are numerous and their peak value varies in function of the loudspeaker and microphone locations. In case the microphone is placed in a pressure node of a mode, that associated peak is not observable. Each peak is associated to the pressure of a particular acoustic mode excited at that particular frequency. The peak height is influenced by the microphone location. The FRFs pressure peaks can be identified by observing the modal simulation.

The validation of the pressure variation for a couple of acoustic modes is performed in the sequel. Let us measure the pressure variation along important directions of some acoustic modes. Firstly we experimentally locate the frequency peak of the observed acoustic mode, in a frequency band that includes the frequency value resulted from simulation. The profiled aluminum slide bar is mounted almost horizontally (OX axis) along the first acoustic mode. Sweep sine waves from 125 Hz to 175 Hz, around the frequency of the first acoustic mode of 152 Hz (from simulation), are generated repeatedly.

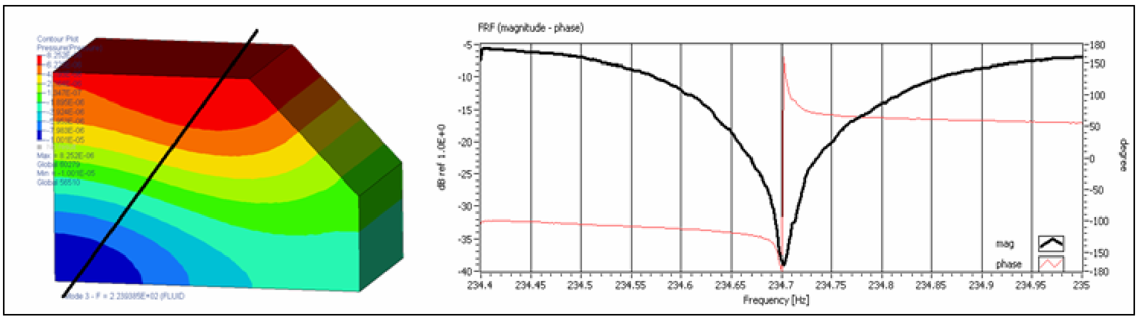

Fig. 11 – Mode #3 [001]: simulation (FEA) and the measured FRF.

For each sweep sine a different microphone position along the slide bar is chosen. For each one a different FRF between the microphone and the speaker, is recorded. An important pressure peak, the closest to 152 Hz (simulation), is constantly observed at 159 Hz. The peak amplitude is low at the middle of the slide and is increasing in amplitude as long as the microphone is moving toward the cavity walls on both sides. In order to collect a continuous pressure variation of the acoustic mode [100], the generated sweep sine wave is very narrow while containing the target (measured) frequency. For the third mode [001] at 234.7Hz, the sweep sine frequency interval it was from 234.4 to 235 Hz (Fig.11). This insures that the standing wave associated to the acoustic mode of interest is continuously excited while the microphone is sliding all along the slide bar. The microphone is dragged manually with constant velocity from exterior by using the ribbon. The pressure variation along the slide bar (indicated by an inclined black segment) is shown in Fig. 11. The pressure node is registered at the middle of the slide bar (the middle of the microphone course). The nodal surface of this mode is marked by the green color (simulation, Fig. 11). By using a similar procedure the pressure variation along the acoustic mode #5, [200], 273 Hz on simulation (uncoupled) and 281 Hz on measurement (coupled), is shown in Fig. 12, where the inclined bar segment is the slide bar position. The two pressure nodes and the pressure peak in the middle of the course (the middle of the slide bar), are visible in the graph. The pressure of the middle peak (blue area) is not so high as at the margins of the slide bar (red areas) because the dark blue area (up-right corner) is not traversed by the microphone sliding on the bar. Hiding the blue zone of the simulation the two surfaces of zero pressure can be seen. The hidden volume has the same pressure sign all over the area and the visible pressure area is of the opposite sign. The microphone records the pressure effective value this being the reason that we observe three lobes. In case we intend to observe a tangential acoustic mode, the slide bar will be placed horizontally (along OY direction) and then vertically. The vertical zero pressure plane will be intersected and the horizontal zero pressure surface too.

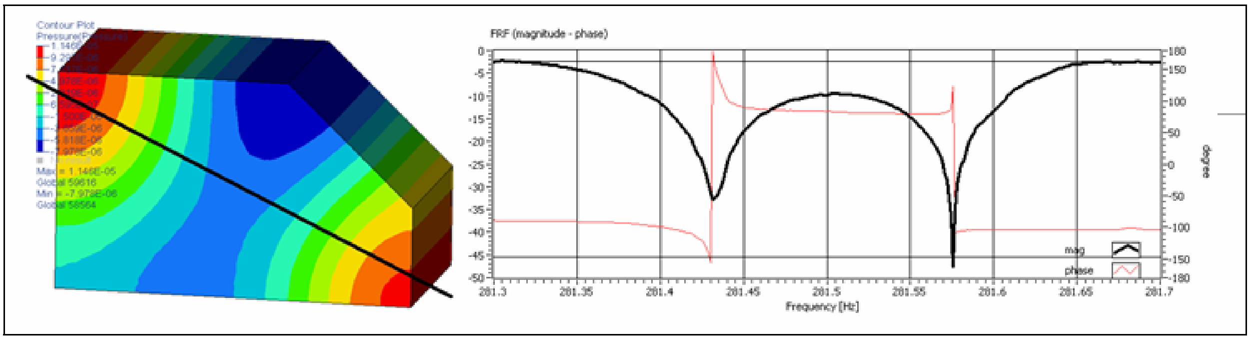

Fig. 12 – Mode # 5, 273 Hz [200], pressure distribution (2 nodes).

5. CONCLUSIONS

The acoustic pressure field of the car cabin is of great importance in improving the habitacle acoustic comfort which is influenced by the acoustic and structural modes of the cabin and the external excitations. A one dimensional fluid-structure coupling system has been presented in order to observe the coupling effect on the uncoupled modes of the structure and the air subsystems. The natural frequencies of both uncoupled subsystems are observed graphically in parallel to the natural frequencies of the coupled system which are the solutions of a derived transcendental equation. In case the air natural frequencies $f_{f,\,n}$ are far from the unique structural natural frequency f_s, the natural frequencies f_i for the entire coupled system are very close to $f_{f,\,n}$ (slightly increased if they are larger and smaller otherwise). For a particular $f_{f,\,n}$ value close to f_s, the associated f_i values differ more from the natural frequencies of the individual subsystems. For a larger damping the deviation of f_i values from $f_{f,\,n}$ value is increased. In case the structural system's natural frequency is altered by changing the mass or the stiffness, the curve is translated along the abscissa while the curve associated to the tube is fixed, hence the intersection points are changing. The study is extended to a simplified car cabin in which the enclosure (structure) is coupled with the air. By using finite element simulation a reduced set of uncoupled acoustic modes and a reduced set of structural modes are obtained. These two sets of uncoupled modes, are used to simulate frequency response functions of the coupled system in order to evaluate the pressure at the comfort points of the habitacle as a response to excitations. The uncoupled (structural and acoustic) modes are employed when the frequency response functions are derived based on the modal version instead of the direct solution. The paper presents a method to experimentally validate and to gain confidence on the simulated acoustic modes by measuring the pressure variation along linear paths across the cabin for the selected acoustic mode. An acquisition system is used to measure narrow band frequency response functions in order to validate the eigenfrequency, the pressure distribution and to point out nodes and pressure peaks along the selected lines traversing the air volume when an acoustic mode is excited.

REFERENCES

1. Coroian, A., Lupea, I., *Improving the sound pressure level for a simplified passenger cabin by using modal participation and size optimization*, Romanian Journal of Acoustics and Vibration, **X**, *1*, pp.100–106, 2013.
2. Jun, Z., and all, *Acoustic design optimization for vibration of cylinder container coupled with interior acoustic field*, JSV, 2009.
3. Luo, J., Gea, H.C., *Modal sensitivity analysis of coupled acoustic-structural systems*, Journal Vibration Acoustics, **119**, 1997.
4. Lupea, I., *Considerations on an elementary fluid-structure coupling system*, Acta Technica Napocensis, Series: Applied Mathematics and Mechanics, **57**, *4*, 2014.
5. Lupea, I., Coroian, A., *Considerations on the Vehicle Floor Carpet Vibro-Acoustic Modelling*, Acta Technica Napocensis, Series: Applied Mathematics and Mechanics, **56**, *II*, pp. 263–268, 2013.
6. Lupea, I., *Considerations on the Helmholtz resonator-simulation and experiment*, Proceedings of the Romanian Academy, Series A, **13**, *2*, pp. 118–124, 2012.
7. Lupea, I., Tibrea Roxana, *Acoustic normal modes simulation of a classroom*, Acta Technica Napocensis, series App. Math. and Mech., **54**, *IV*, 2011.
8. Lupea, I., Szathmari, R., *Vibroacoustic frequency response on a passenger compartment*, Journal of Vibroengineering (Kaunas, Lithuania), **12**, *4*, 2010.
9. Lupea, I., Cormier, J., *Size and shape optimization of a polymeric impact energy absorber by simulation*, Materiale Plastice, **44**, *4*, pp. 339–344, 2007.
10. Nefske, D.J., Wolf, J.A., Howell, L., *Structural-acoustic finite element analysis of the automobile passenger compartment: a review of current practice*, Journal of Sound and Vibration (JSV), **80**, *2*, pp. 247–266, 1982.
11. Reed, C., *Application of Optistruct optimization to body in white design*, Altair Engineering Ltd, 2002.
12. Sheng, G., *Vehicle noise vibration and sound quality*, SAE International, Warrendale, USA, 2012.
13. HyperWorks – Optistruct, Altair Engineering, Troy, MI, USA, 2010.
14. Labview, National Instruments, Austin, Texas, USA.

Received September 21, 2015